

REGULARIZED RECONSTRUCTION OF ULTRASONIC IMAGING AND THE REGULARIZATION PARAMETER CHOICE

Leonardo G. S. Zanin, Fábio K. Schneider and Marcelo V. W. Zibetti

Graduate School of Electrical Engineering and Computer Science, Federal University of Technology, Paraná, Brazil

Keywords: Ultrasound imaging, Inverse problems, Image reconstruction, Singular value decomposition.

Abstract: Ultrasound image reconstruction based on inverse problems has attracted attention to the ultrasonic imaging research community recently. Different from standard beamforming-based methods techniques, this new imaging method tries to solve a linear system $g=Hf$ as a form of reconstructing the ultrasound image. In order to understand the behaviour of this imaging system, it is important to analyse the forward problem. In this paper, we analyse the effect of the noise in acquisition matrix using singular value decomposition. Also, the effect of regularization parameter in dealing with the noise is investigated in regularized. This analysis provides some interesting insights in the understanding of how the inverse reconstruction can be improve some aspects higher than beamforming.

1 INTRODUCTION

Beamforming-based methods are traditionally used to ultrasound imaging, which relies on Delay-And-Sum (DAS) approach (Stergiopoulos, 2000). The DAS approach provides some positive benefits such as real-time imaging. Even though Beamforming (BF) has had some important improvements, such as adaptive BF (Synnevåg et al., 2007) it still has limitations on its achieved resolution. Going further may require new reconstruction approaches.

Some recent research such (Lavarello et al., 2006); (Lingvall and Olofsson, 2007); (Viola et al., 2008), proposed an ultrasonic image reconstruction methods based on inverse problems (Barrett and Myers, 2004). In this methodology the data acquisition process, know as forward system, is utilized to relate the image of a region of interest (ROI) with the captured data-signal. The reconstructed image is obtained by solving this system, what is known as the inverse solution (Barrett and Myers, 2004).

Inverse approaches can significantly reduce the point spreading, providing a sharper image with increased quality and resolution (Lavarello et al., 2006); (Lingvall and Olofsson, 2007); (Viola et al., 2008). The noise, however, may limit the potential of the inverse reconstruction, so a proper balance

must be applied. The regularized reconstructions (RR) treat this problem by choosing an adequate regularization parameter (Hansen, 1998); (Vogel, 2002).

Several methods for optimal automatic determination of this parameter exist, such as GCV (Golub and Von Matt, 1997), L-curve and others (Hansen, 1998). However, automatic determination of the parameter highly increases the computational cost of the reconstruction. Other alternatives are prior determination of the regularization, instead of automatic, such as the statistical methods (Bovik, 2000).

This paper proposes a combination of RR and prior choice of the regularization parameter to ultrasonic imaging systems. The paper is organized as following: in Section 2, the forward system is explained, in Section 3, the RR is presented, together with the choice of the regularization parameter. In Section 4, a small brief of the Singular Value Decomposition (SVD), and the spectrums of the image and noise are presented. The analysis of the system for the prior choice of the regularization parameter is presented in Section 5, together with some samples of reconstructed images. Finely, in Section 6, a discussion of the results and the conclusions are drawn.

2 FORWARD SYSTEM FOR ULTRASOUND IMAGING

The investigation acoustic pulse in the spatial position \mathbf{r} , during a time t , is models as (Lingvall and Olofsson, 2007):

$$p(\mathbf{r}, t) = \sum_{k=1}^K h_k^{sf}(\mathbf{r}, t) * h_k^{ef}(t) * u_k(t) \quad (1)$$

In (1), its considered K elements in the ultrasound array. The $u_k(t)$ is the electric signal applied to the k^{th} array element, $h_k^{ef}(t)$ is the forward electro-acoustic impulse response of the element, while the acoustic spatial impulse response is denoted as $h_k^{sf}(\mathbf{r}, t)$. The pressure $p(\mathbf{r}, t)$ reaching a position \mathbf{r} react according to the reflectivity function $f(\mathbf{r})$, which is the information to be imaged. This echo signal formed by this interaction at the position \mathbf{r} , reaching the n^{th} array element is:

$$g_n(\mathbf{r}, t) = h_n^{sb}(\mathbf{r}, t) * h_n^{eb}(t) * p(\mathbf{r}, t) f(\mathbf{r}) \quad (2)$$

We consider that N_e elements in the array are used for echo recording. This returning echo is spread by the backward spatial impulse response $h_n^{sb}(\mathbf{r}, t)$, reaching the sensor where it is convolved with the backward electro-acoustic impulse response $h_n^{eb}(t)$. Joining (1) and (2) we can express the echo from a particular position as:

$$g_n(\mathbf{r}, t) = h_n(\mathbf{r}, t) f(\mathbf{r}) \quad (3)$$

where

$$h_n(\mathbf{r}, t) = h_n^{sb}(\mathbf{r}, t) * h_n^{eb}(t) * p(\mathbf{r}, t) \quad (4)$$

Considering that the data-signal $g_n(\mathbf{r}, t)$ from (3) is provided by echoes from all \mathbf{r} positions belonging to the Cartesian coordinates in the 2D image grid. In this paper we assume that the discrete signal can be represented as:

$$g_n[\mathbf{r}, t_i] = \sum_{\mathbf{r} \in \text{grid}} h_n[\mathbf{r}, t_i] f[\mathbf{r}] \quad (5)$$

The image size is $M_1 \times M_2$, being $M = M_1 \cdot M_2$ number of pixels. Also, t_i is a discrete time sample being S the total time samples from an element. Putting the equation (5) in a matrix-vector format leads to $\mathbf{g}_n = \mathbf{H}_n \mathbf{f}$, where $\mathbf{g}_n = [g_n(t_1), \dots, g_n(t_S)]^T$ is a vector with all the captured samples from the n^{th} element, while $\mathbf{f} = [f(1,1), \dots, f(M_1,1), f(1,2), \dots, f(M_1, M_2)]^T$ is a vector with the image pixels re-ordered.

We can join the time samples from all elements in the form:

$$\mathbf{g} = \mathbf{H} \mathbf{f} + \boldsymbol{\eta} = \begin{bmatrix} \mathbf{g}_1 \\ \vdots \\ \mathbf{g}_N \end{bmatrix} = \begin{bmatrix} \mathbf{H}_1 \\ \vdots \\ \mathbf{H}_N \end{bmatrix} \mathbf{f} + \boldsymbol{\eta} \quad (6)$$

In (6), we have the full system. The \mathbf{H} matrix has size of $N \times M$, being $N = N_e \cdot S$. The sensor response, pulses and signal spreading are all involved to form the matrix, so it contains the system behavior. The noise is represented by $\boldsymbol{\eta}$.

3 REGULARIZED RECONSTRUCTION

The RR used in this paper is based on the Tikhonov regularization for least squares (Hansen, 1998), described as:

$$\hat{\mathbf{f}}_{Tik}(\alpha) = \arg \min_{\mathbf{f}} \left[\|\mathbf{g} - \mathbf{H} \mathbf{f}\|_2^2 + \alpha^2 \|\mathbf{f}\|_2^2 \right] \quad (7)$$

In (7), the parameter α , known as the regularization parameter, is real and positive (Bovik, 2000). When $\alpha \rightarrow 0$, the reconstructed image is usually sharp, but noise is amplified due to the ill-conditioning of \mathbf{H} . Increasing the regularization parameter reduces noise amplification, stabilizing the image. However, it also reduces the sharpness of the solution.

The minimum of (7) is achieved when the gradient is zero, or equivalently when:

$$(\mathbf{H}^T \mathbf{H} + \alpha^2 \mathbf{I}) \hat{\mathbf{f}}_{Tik} = \mathbf{H}^T \mathbf{g} \quad (8)$$

This gives the following solution:

$$\hat{\mathbf{f}}_{Tik} = (\mathbf{H}^T \mathbf{H} + \alpha^2 \mathbf{I})^{-1} \mathbf{H}^T \mathbf{g} \quad (9)$$

The reconstruction in (9) requires the inversion of the matrix; however, this computation can be done off-line and then stored in the ultrasound equipment to reconstruction process. On the other hand, prior choices of α must be defined previously to the inverse computation.

3.1 Choice of the Regularization Parameter

Automatic parameter selection methods, such as the GCV (Golub and Von Matt, 1997) and the L-curve (Hansen, 1998), are alternatives to the balance between noise and image sharpness, but they cannot determine the parameter *a priori*.

Our alternative for prior α determination requires previous knowledge of the noise levels. Several methods based on the knowledge of the noise and

image variances exist, such as the statistical Maximum a Posterior (MAP) estimation (Mohammad-Djafari, 1995); (Therrien, 1992). MAP estimation leads to a reconstruction algorithm similar to (7), where $\alpha = \delta_\eta / \delta_f$, being δ_η and δ_f the noise and the image standard deviation respectively.

In (Hansen, 1998) it is mentioned that the regularization is needed if the discrete Picard condition is not achieved. In order to clearly state the discrete Picard condition, we briefly mention the SVD and define the spectrums of the image and noise.

4 THE SINGULAR VALUE ANALYSIS

4.1 Singular Value Decomposition

The SVD (Barrett and Myers, 2004) is able to reveal the spectrum of a matrix by diagonalizing it. The spectrum shows the filtering effect of the acquisition system. This information is similar to the frequency response of shift invariant systems.

Utilizing the SVD, the matrix \mathbf{H} can be represented as:

$$\mathbf{H} = \mathbf{U}\mathbf{S}\mathbf{V}^T = \sum_{k=1}^p \sigma_k \mathbf{u}_k \mathbf{v}_k^T \quad (10)$$

Where \mathbf{U} is a $N \times N$ matrix, \mathbf{V} is a $M \times M$ matrix, and \mathbf{S} is an $N \times M$ diagonal matrix with the elements $\sigma_1, \sigma_2, \dots, \sigma_p$, where $p = \min(N, M)$ in its diagonal. The orthonormal columns \mathbf{v}_k represent the right singular vectors. The orthonormal matrix \mathbf{V}^T transforms the image vector \mathbf{f} to new space where the singular values weight this transformed image. The result is transformed to another space by the \mathbf{U} matrix, constructed with orthonormal column vectors \mathbf{u}_k , which are the left singular vectors. The set $\{\sigma_k, \mathbf{u}_k, \mathbf{v}_k\}$, $1 \leq k \leq p$, are the singular system of \mathbf{H} .

4.2 Definition of the Spectrums of the Image and the Noise

Using the SVD one can observe that the operation $\mathbf{H}\mathbf{f}$ first transforms the image to the spectral space, through $\mathbf{V}^T\mathbf{f}$, forming the coefficients $\{\mathbf{v}_k^T\mathbf{f}\}$, $1 \leq k \leq p$, which is the unfiltered spectrum of image. In the spectrum, the image is filtered through $\mathbf{S}\mathbf{V}^T\mathbf{f}$ generating the noiseless data spectrum (filtered spectrum) defined by $\{\sigma_k(\mathbf{v}_k^T\mathbf{f})\}$, $1 \leq k \leq p$. The same filtered spectrum can be obtained by $\mathbf{U}^T\mathbf{H}\mathbf{f}$,

generating $\{\mathbf{u}_k^T\mathbf{H}\mathbf{f}\}$, $1 \leq k \leq p$, which is the same as $\{\sigma_k(\mathbf{v}_k^T\mathbf{f})\}$. Also, we can observe the filtered spectrum with noise, resulted from $\mathbf{g} = \mathbf{H}\mathbf{f} + \boldsymbol{\eta}$, by doing $\mathbf{U}^T\mathbf{g} = \mathbf{U}^T\mathbf{H}\mathbf{f} + \mathbf{U}^T\boldsymbol{\eta}$ which is a composition of filtered image spectrum, or $\mathbf{U}^T\mathbf{H}\mathbf{f}$, and the noise spectrum, or $\mathbf{U}^T\boldsymbol{\eta}$, also defined as $\{\mathbf{u}_k^T\boldsymbol{\eta}\}$, $1 \leq k \leq p$.

In general, the image spectrum is relatively arbitrary. However the filtered spectrum is more predictable. According to the discrete Picard condition (Hansen, 1998), the absolute value of the filtered image spectrum, or $\sigma_k|\mathbf{v}_k^T\mathbf{f}|$, must decay, on average, at the same rate (or more) than the rate of decaying of the s.v. (Hansen, 1998); (Vogel, 2002). This behavior, which is stated for general systems, is also observed for ultrasonic systems.

4.3 Prior Determination of the Regularization Parameter

The regularization is needed because the inverse will strongly amplify the components related to small singular values. One can say those spectrum components on elevated k positions may have more noise than signal, while the lower k positions may have more signal than noise.

The regularized reconstruction, expressed with the SVD is:

$$\hat{\mathbf{f}}_{Tik} = (\mathbf{H}^T\mathbf{H} + \alpha^2\mathbf{I})^{-1}\mathbf{H}^T\mathbf{g} = \sum_{k=1}^p \frac{\sigma_k(\mathbf{u}_k^T\mathbf{g})}{\sigma_k^2 + \alpha^2} \mathbf{v}_k \quad (11)$$

One can note that the RR, instead of inverting the s.v. directly, invert the regularized s.v., or $\sqrt{\sigma_k^2 + \alpha^2}$. This stabilizes the inverse solution, avoiding excessive noise amplification, and corrects the filtered signal when the signal is stronger than noise.

Our main contribution in this paper is the observation that the regularized s.v. must follow the average decaying of data spectrum. The data spectrum (noise plus filtered spectrum) follows, on average, the regularized s.v. line, or:

$$\left| \mathbf{u}_k^T\mathbf{g} \right| / o \approx \sqrt{\sigma_k^2 + \alpha^2} \quad (12)$$

Considering the weighting by a constant o , the α is δ_η / o , which is very consistent with MAP, where the constant o is chosen as δ_f . So, in order to find a reasonable regularization parameter a priori, one may use data captured from several different study objects, i.e. phantoms. This data can be transformed to the spectrum, using the SVD, and an appropriate scaling constant o can be found. One may simply adjust the curve manually so the constant o may provide the overlap between singular values and data

spectrum, especially in the lower k components.

5 SIMULATION RESULTS

In this section, the reconstructed images with regularized inversion using different parameters are shown. For these experiments we used signals generated using Field II toolbox (Jensen, 1996). For all experiments an ultrasonic pulse of 5 MHz, with 80% of the bandwidth, sampled at 100MHz and sound speed of $c=1540$ m/s were considered. The ROI is an area of 10×10 mm in which the sensor array is 25mm from the center of the ROI in the longitudinal dimension, and centered in the lateral dimension. The 64 elements of the sensor are spaced by $\lambda=c/f$. We do not use focused pulses, neither any non-uniform apodization. The resolution grid is 60×60 pixels. Some sample figures are reconstructed with BF and RR from (9). Also, we add a white Gaussian noise to the signal with standard deviation to achieve a SNR of 10dB and 20dB.

The Figure 1 has the results of the determination of the ideal α for this system. Note that average noise lines for both SNR of 10dB and 20dB, cross the singular values line. This means we need to regularize the system to avoid excessive noise amplification. The standard deviation for the noise and acquisition with SNR of 10 and 20dB are shown in Table 1. By adjusting the curves the estimated constant o is nearly to $3 \cdot 10^{-2}$, which is close to the α parameter suggested by MAP estimation. The regularized curves are plotted in the Figure 1.

Table 1: Standard deviation and regularization parameter.

SNR	$\delta_{\eta}(10^{-11})$	$\alpha(10^{-9})$
10dB	6.5652	2.1884
20dB	2.0786	0.6928

In order to compare the RR with different parameters for both SNR's, we utilized three α spanned by one order of magnitude above an one order of magnitude below, i.e., $\alpha_{\text{below}}=0.1 \times \alpha$, α , and $\alpha_{\text{above}}=10 \times \alpha$. The results are shown in Figure 2, comparing with the BF reconstruction.

Analyzing the results, it is possible to observe in the images reconstructed with α_{below} , in figures 2(a) and (e), that the noise were over amplified. With the ideal α , the inverse results have a noise level between the underregularized and BF. The noise was not too much amplified and the spots are more compact, which corresponds to an improvement in resolution. Figures 2(c) and (g) show reconstructed images obtained by α_{above} , which is an overregularized

inverse approach. This result is more similar to BF, but it is possible to note that the spots are not so spread as BF. Comparing these inverse reconstructions with the BF, is possible to note that the noise was amplified, but the spreading was significantly reduced.

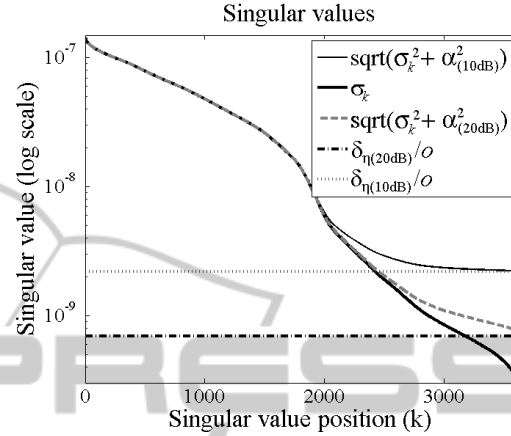


Figure 1: The singular values σ_k , the average noise level δ_{η}/o , and the regularized singular values $\text{sqrt}(\sigma_k^2 + \alpha^2)$ adjusted for SNR of 10dB and 20dB.

6 DISCUSSIONS AND CONCLUSIONS

This analysis evidenced the importance of choice of regularization parameter. The higher the α , smaller the noise and smaller the reduction of spreading; the smaller the α , higher the correction of the spreading under the cost of increased noise amplification. With RR, an improvement in image resolution was obtained when compared with DAS BF.

In this paper we also investigate how the noise affects the ultrasound forward system through de SVD analysis. Mainly, we use this analysis to obtain a better regularization parameter to regularized inverse approach. We observed some of advantage that inverse reconstruction provides when applied to ultrasound imaging systems. This new method, also investigated in recent works (Lavarello et al., 2006); (Lingvall and Olofsson, 2007); (Viola et al., 2008) has been proven its effectiveness and is able to be used in modern ultrasound systems.

Some of limitations existent in BF, such as the lateral spreading of the spots are improved with this new method. The great limitation of RR is the computational cost and memory requirements, which makes it, by now, impossible to be applied for real-time imaging as BF. However their ability of improve the ultrasound image resolution makes it

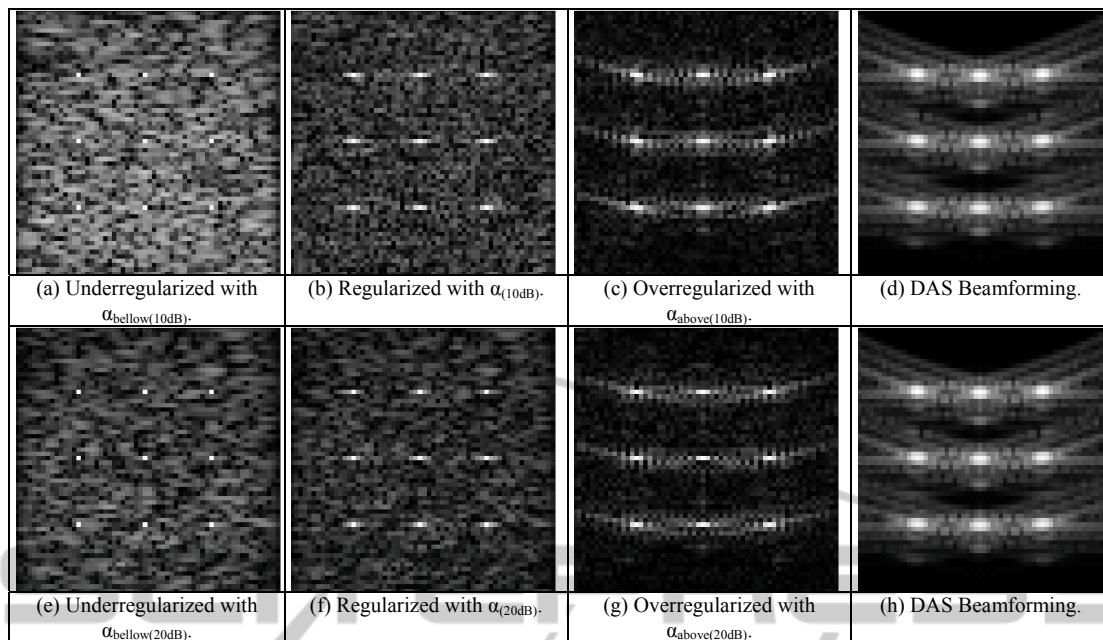


Figure 2: Images obtained for reconstructions of the data with SNR of 10 (a-d) and 20dB (e-h), through the regularized inverse, obtained from different α and DAS Beamforming.

very attractive and researches in this area must be encouraged.

ACKNOWLEDGEMENTS

Authors thanks the Brazilian Federal Agency for Post-Graduate Education (CAPES) for financial support.

REFERENCES

- Barrett, H. H., & Myers, K. J. M. (2004). *Foundations of Image Science*. John Wiley & Sons.
- Bovik, A. C. (2000). *Handbook of image and video processing*. Academic Press.
- Golub, G. H., & Von Matt, U. (1997). Generalized cross-validation for large-scale problems. *Journal of Computational and Graphical Statistics*, 1–34. JSTOR.
- Hansen, P. C. (1998). *Rank-deficient and discrete ill-posed problems*. SIAM.
- Jensen, J. A. (1996). Field: A Program for Simulating Ultrasound Systems Field: A Program for Simulating Ultrasound Systems. *Medical & Biological Engineering & Computing* (Vol. 34, pp. 351- 353).
- Lavarello, R. J., Kamalabadi, F., & O'Brien, W. D. (2006). A Regularized Inverse Approach to Ultrasonic Pulse-Echo Imaging. *IEEE Transactions on Medical Imaging*, 25(6), 712-22.
- Lingvall, F., & Olofsson, T. (2007). On time-domain model-based ultrasonic array imaging. *IEEE Transactions on Ultrasonics, Ferroelectrics and Frequency Control*, 54(8), 1623-33.
- Mohammad-Djafari, A. (1995). A full Bayesian approach for inverse problems. *International Workshop on Maximum Entropy and Bayesian Methods*, 135-144.
- Stergiopoulos, S. (2000). *Advanced Signal Processing Handbook: Theory and Implementation for Radar, Sonar, and Medical Imaging Real Time Systems*. Abingdon: CRC Press.
- Synnevåg, J.-F., Austeng, A., & Holm, S. (2007). Adaptive Beamforming Applied to Medical Ultrasound Imaging. *IEEE Transactions on Ultrasonics, Ferroelectrics and Frequency Control*, 54(8), 1606-13.
- Therrien, C. W. (1992). *Discrete Random Signals and Statistical Signal Processing*. Prentice Hall.
- Viola, F., Ellis, M., & Walker, W. F. (2008). Time-domain optimized near-field estimator for ultrasound imaging: initial development and results. *IEEE Transactions on Medical Imaging*, 27(1), 99-110. doi:10.1109/TMI.2007.903579
- Vogel, C. R. (2002). *Computational Methods for Inverse Problems*. SIAM.